

University of Kentucky  
UKnowledge

Physics and Astronomy Faculty Publications

Physics and Astronomy

4-7-2014

# Single Spin Asymmetries of Inclusive Hadrons Produced in Electron Scattering from a Transversely Polarized $^3\text{He}$ Target

K. Allada

*Massachusetts Institute of Technology*

Y. X. Zhao

*University of Science and Technology of China, China*

K. Aniol

*California State University - Los Angeles*

J. R. M. Annand

*University of Glasgow, United Kingdom*

T. Averett

*College of William and Mary**See next page for additional authors*

Right click to open a feedback form in a new tab to let us know how this document benefits you.  
Follow this and additional works at: [https://uknowledge.uky.edu/physastron\\_facpub](https://uknowledge.uky.edu/physastron_facpub)

Part of the [Astrophysics and Astronomy Commons](#), and the [Physics Commons](#)

## Repository Citation

Allada, K.; Zhao, Y. X.; Aniol, K.; Annand, J. R. M.; Averett, T.; Benmokhtar, F.; Bertozzi, W.; Bradshaw, P. C.; Bosted, P.; Camsonne, A.; Dutta, C.; Kolarkar, Ameya Suresh; and Korsch, Wolfgang, "Single Spin Asymmetries of Inclusive Hadrons Produced in Electron Scattering from a Transversely Polarized  $^3\text{He}$  Target" (2014). *Physics and Astronomy Faculty Publications*. 127.  
[https://uknowledge.uky.edu/physastron\\_facpub/127](https://uknowledge.uky.edu/physastron_facpub/127)

This Article is brought to you for free and open access by the Physics and Astronomy at UKnowledge. It has been accepted for inclusion in Physics and Astronomy Faculty Publications by an authorized administrator of UKnowledge. For more information, please contact [UKnowledge@lsv.uky.edu](mailto:UKnowledge@lsv.uky.edu).

---

**Authors**

K. Allada, Y. X. Zhao, K. Aniol, J. R. M. Annand, T. Averett, F. Benmokhtar, W. Bertozzi, P. C. Bradshaw, P. Bosted, A. Camsonne, C. Dutta, Ameya Suresh Kolarkar, and Wolfgang Korsch

**Single Spin Asymmetries of Inclusive Hadrons Produced in Electron Scattering from a Transversely Polarized  $^3\text{He}$  Target****Notes/Citation Information**

Published in *Physical Review C: Nuclear Physics*, v. 89, article 042201(R), p. 1-6.

©2014 American Physical Society

The copyright holder has granted permission for posting the article here.

Due to the large number of authors involved, only the first 10 and the ones affiliated with the University of Kentucky are listed in the author section above. The authors of this article are collectively known as Jefferson Lab Hall A Collaboration.

**Digital Object Identifier (DOI)**

<http://dx.doi.org/10.1103/PhysRevC.89.042201>

## Single spin asymmetries of inclusive hadrons produced in electron scattering from a transversely polarized $^3\text{He}$ target

K. Allada,<sup>1,2,\*</sup> Y. X. Zhao,<sup>3</sup> K. Aniol,<sup>4</sup> J. R. M. Annand,<sup>5</sup> T. Averett,<sup>6</sup> F. Benmokhtar,<sup>7</sup> W. Bertozzi,<sup>1</sup> P. C. Bradshaw,<sup>6</sup> P. Bosted,<sup>2</sup> A. Camsonne,<sup>2</sup> M. Canan,<sup>8</sup> G. D. Cates,<sup>9</sup> C. Chen,<sup>10</sup> J.-P. Chen,<sup>2</sup> W. Chen,<sup>11</sup> K. Chirapatpimol,<sup>9</sup> E. Chudakov,<sup>2</sup> E. Cisbani,<sup>12,13</sup> J. C. Cornejo,<sup>4</sup> F. Cusanno,<sup>14</sup> M. Dalton,<sup>9</sup> W. Deconinck,<sup>1</sup> C. W. de Jager,<sup>2</sup> R. De Leo,<sup>15</sup> X. Deng,<sup>9</sup> A. Deur,<sup>2</sup> H. Ding,<sup>9</sup> P. A. M. Dolph,<sup>9</sup> C. Dutta,<sup>16</sup> D. Dutta,<sup>17</sup> L. El Fassi,<sup>18</sup> S. Frullani,<sup>14,13</sup> H. Gao,<sup>11</sup> F. Garibaldi,<sup>14,13</sup> D. Gaskell,<sup>2</sup> S. Gilad,<sup>1</sup> R. Gilman,<sup>2,18</sup> O. Glamazdin,<sup>19</sup> S. Golge,<sup>8</sup> L. Guo,<sup>20</sup> D. Hamilton,<sup>5</sup> O. Hansen,<sup>2</sup> D. W. Higinbotham,<sup>2</sup> T. Holmstrom,<sup>21</sup> J. Huang,<sup>1,20</sup> M. Huang,<sup>11</sup> H. F. Ibrahim,<sup>22</sup> M. Iodice,<sup>23</sup> X. Jiang,<sup>18,20</sup> G. Jin,<sup>9</sup> M. K. Jones,<sup>2</sup> J. Katich,<sup>6</sup> A. Kelleher,<sup>6</sup> W. Kim,<sup>24</sup> A. Kolarkar,<sup>16</sup> W. Korsch,<sup>16</sup> J. J. LeRose,<sup>2</sup> X. Li,<sup>25</sup> Y. Li,<sup>25</sup> R. Lindgren,<sup>9</sup> N. Liyanage,<sup>9</sup> E. Long,<sup>26</sup> H.-J. Lu,<sup>3</sup> D. J. Margaziotis,<sup>4</sup> P. Markowitz,<sup>27</sup> S. Marrone,<sup>15</sup> D. McNulty,<sup>28</sup> Z.-E. Meziani,<sup>29</sup> R. Michaels,<sup>2</sup> B. Moffit,<sup>1,2</sup> C. Muñoz Camacho,<sup>30</sup> S. Nanda,<sup>2</sup> A. Narayan,<sup>17</sup> V. Nelyubin,<sup>9</sup> B. Norum,<sup>9</sup> Y. Oh,<sup>31</sup> M. Osipenko,<sup>32</sup> D. Parno,<sup>7</sup> J.-C. Peng,<sup>33</sup> S. K. Phillips,<sup>34</sup> M. Posik,<sup>29</sup> A. J. R. Puckett,<sup>1,20</sup> X. Qian,<sup>35</sup> Y. Qiang,<sup>11,2</sup> A. Rakhman,<sup>36</sup> R. Ransome,<sup>18</sup> S. Riordan,<sup>9</sup> A. Saha,<sup>2,†</sup> B. Sawatzky,<sup>29,2</sup> E. Schulte,<sup>18</sup> A. Shahinyan,<sup>37</sup> M. H. Shabestari,<sup>9</sup> S. Širca,<sup>38</sup> S. Stepanyan,<sup>39</sup> R. Subedi,<sup>9</sup> V. Sulkosky,<sup>1,2</sup> L.-G. Tang,<sup>10</sup> A. Tobias,<sup>9</sup> G. M. Urciuoli,<sup>14</sup> I. Vilaridi,<sup>15</sup> K. Wang,<sup>9</sup> Y. Wang,<sup>33</sup> B. Wojtsekhowski,<sup>2</sup> X. Yan,<sup>3</sup> H. Yao,<sup>29</sup> Y. Ye,<sup>3</sup> Z. Ye,<sup>10</sup> L. Yuan,<sup>10</sup> X. Zhan,<sup>1</sup> Y. Zhang,<sup>40</sup> Y.-W. Zhang,<sup>40</sup> B. Zhao,<sup>6</sup> X. Zheng,<sup>9</sup> L. Zhu,<sup>33,10</sup> X. Zhu,<sup>11</sup> and X. Zong<sup>11</sup>

(Jefferson Lab Hall A Collaboration)

<sup>1</sup>Massachusetts Institute of Technology, Cambridge, Massachusetts 02139, USA

<sup>2</sup>Thomas Jefferson National Accelerator Facility, Newport News, Virginia 23606, USA

<sup>3</sup>University of Science and Technology of China, Hefei 230026, People's Republic of China

<sup>4</sup>California State University, Los Angeles, Los Angeles, California 90032, USA

<sup>5</sup>University of Glasgow, Glasgow G12 8QQ, Scotland, United Kingdom

<sup>6</sup>College of William and Mary, Williamsburg, Virginia 23187, USA

<sup>7</sup>Carnegie Mellon University, Pittsburgh, Pennsylvania 15213, USA

<sup>8</sup>Old Dominion University, Norfolk, Virginia 23529, USA

<sup>9</sup>University of Virginia, Charlottesville, Virginia 22904, USA

<sup>10</sup>Hampton University, Hampton, Virginia 23187, USA

<sup>11</sup>Duke University, Durham, North Carolina 27708, USA

<sup>12</sup>INFN, Sezione di Roma, I-00185 Rome, Italy

<sup>13</sup>Istituto Superiore di Sanità, I-00161 Rome, Italy

<sup>14</sup>INFN, Sezione di Roma, I-00161 Rome, Italy

<sup>15</sup>INFN, Sezione di Bari and University of Bari, I-70126 Bari, Italy

<sup>16</sup>University of Kentucky, Lexington, Kentucky 40506, USA

<sup>17</sup>Mississippi State University, Mississippi State, Mississippi 39762, USA

<sup>18</sup>Rutgers, State University of New Jersey, Piscataway, New Jersey 08855, USA

<sup>19</sup>Kharkov Institute of Physics and Technology, Kharkov 61108, Ukraine

<sup>20</sup>Los Alamos National Laboratory, Los Alamos, New Mexico 87545, USA

<sup>21</sup>Longwood University, Farmville, Virginia 23909, USA

<sup>22</sup>Cairo University, Giza 12613, Egypt

<sup>23</sup>INFN, Sezione di Roma Tre, I-00146 Rome, Italy

<sup>24</sup>Kyungpook National University, Taegu 702-701, Republic of Korea

<sup>25</sup>China Institute of Atomic Energy, Beijing, People's Republic of China

<sup>26</sup>Kent State University, Kent, Ohio 44242, USA

<sup>27</sup>Florida International University, Miami, Florida 33199, USA

<sup>28</sup>University of Massachusetts, Amherst, Massachusetts 01003, USA

<sup>29</sup>Temple University, Philadelphia, Pennsylvania 19122, USA

<sup>30</sup>Université Blaise Pascal/IN2P3, F-63177 Aubière, France

<sup>31</sup>Seoul National University, Seoul, South Korea

<sup>32</sup>INFN, Sezione di Genova, I-16146 Genova, Italy

<sup>33</sup>University of Illinois, Urbana-Champaign, Illinois 61801, USA

<sup>34</sup>University of New Hampshire, Durham, New Hampshire 03824, USA

<sup>35</sup>Physics Department, Brookhaven National Laboratory, Upton, New York, USA

<sup>36</sup>Syracuse University, Syracuse, New York 13244, USA

<sup>37</sup>Yerevan Physics Institute, Yerevan 375036, Armenia

<sup>38</sup>University of Ljubljana, SI-1000 Ljubljana, Slovenia<sup>39</sup>Kyungpook National University, Taegu City, South Korea<sup>40</sup>Lanzhou University, Lanzhou 730000, Gansu, People's Republic of China

(Received 29 October 2013; published 7 April 2014)

We report the first measurement of target single spin asymmetries ( $A_N$ ) in the inclusive hadron production reaction,  $e + {}^3\text{He}^\uparrow \rightarrow h + X$ , using a transversely polarized  ${}^3\text{He}$  target. The experiment was conducted at Jefferson Lab in Hall A using a 5.9-GeV electron beam. Three types of hadrons ( $\pi^\pm$ ,  $K^\pm$ , and proton) were detected in the transverse hadron momentum range  $0.54 < p_T < 0.74$  GeV/c. The range of  $x_F$  for pions was  $-0.29 < x_F < -0.23$  and for kaons was  $-0.25 < x_F < -0.18$ . The observed asymmetry strongly depends on the type of hadron. A positive asymmetry is observed for  $\pi^+$  and  $K^+$ . A negative asymmetry is observed for  $\pi^-$ . The magnitudes of the asymmetries follow  $|A^{\pi^-}| < |A^{\pi^+}| < |A^{K^+}|$ . The  $K^-$  and proton asymmetries are consistent with zero within the experimental uncertainties. The  $\pi^+$  and  $\pi^-$  asymmetries measured for the  ${}^3\text{He}$  target and extracted for neutrons are opposite in sign with a small increase observed as a function of  $p_T$ .

DOI: [10.1103/PhysRevC.89.042201](https://doi.org/10.1103/PhysRevC.89.042201)

PACS number(s): 25.30.Fj, 14.20.Dh, 24.85.+p, 25.30.Rw

The study of the transverse single spin asymmetries (TSSAs) is one of the most active areas of research in modern hadronic physics. TSSA is an important tool to advance our understanding of the nucleon spin, to reveal the role of the quark orbital angular momentum (OAM), and to access the three-dimensional structure of the nucleon in momentum space [1]. Current research on TSSA focuses on the polarized proton-proton ( $pp^\uparrow$ ) and lepton-nucleon ( $lN^\uparrow$ ) reaction channels.

An early observation of large left-right SSAs ( $A_N$ ) in the  $pp^\uparrow \rightarrow \pi^\pm X$  reaction by the Fermilab E704 experiment at  $\sqrt{s} = 19.4$  GeV [2,3] revealed a strong dependence on the hadron type. In the center-of-mass frame of the polarized  $pp^\uparrow$  collision, viewed along the momentum direction of the polarized proton,  $\pi^+$  favors the left side of the spin vector, whereas  $\pi^-$  favors the right side of the spin vector. More recently, such nonvanishing TSSAs were observed for  $\pi^\pm$  and  $K^\pm$  at  $\sqrt{s} = 62.4$  GeV by BRAHMS [4], and for neutral pions at  $\sqrt{s} = 200$  GeV by the STAR experiment at RHIC [5]. Although TSSAs have been observed in  $pp^\uparrow$  reactions for more than two decades, measurement in semi-inclusive deep inelastic scattering (SIDIS) is regarded as one of the cleanest ways to understand them at the partonic level. TSSAs have been measured in the SIDIS reaction ( $lp^\uparrow \rightarrow l'hX$ ) by HERMES [6–9] with a polarized proton target and by COMPASS [10–13] using polarized proton and deuteron targets. Recently, they have been measured at Jefferson Lab in Hall A using a polarized  ${}^3\text{He}$  target [14,15].

The origin of TSSAs is currently interpreted using two theoretical approaches [16]. The first approach is based on the transverse-momentum-dependent distribution and fragmentation functions (TMDs) in the framework of the TMD factorization, and is mostly used to explain TSSAs in the SIDIS process. There are two reaction mechanisms: the Collins effect [17] and the Sivers effect [18]. In the Collins effect, the TSSA is generated by the transversity distribution, which represents the probability of finding a transversely polarized parton inside a transversely polarized nucleon, and the Collins fragmentation

function, which correlates the transverse polarization of the quark with the transverse momentum of the outgoing hadron ( $p_T$ ). In the Sivers effect, the TSSA is generated by the Sivers distribution function, which correlates the quark's transverse momentum and the nucleon's spin and is sensitive to the quark OAM. More specifically, the observed asymmetry due to the Sivers function arises from the final-state interaction between the struck quark and the nucleon remnant in SIDIS. On the other hand, the Sivers function in the Drell-Yan process is expected to arise from the initial-state interactions [19]. Taking gauge links into consideration, the Sivers distribution is predicted to be process dependent in the sense that it differs in sign between SIDIS and Drell-Yan processes [19,20]. Furthermore, in models such as the diquark model [21], one can connect the Sivers distribution for each quark to its contribution to the anomalous magnetic moment of the nucleon.

The second approach is based on the twist-3 collinear factorization [22–25], where the SSAs are interpreted in terms of higher-twist quark-gluon correlations, and is mainly used to explain the TSSAs in the  $pp^\uparrow \rightarrow hX$  channel. It was also shown that the TMD factorization and twist-3 methods are related [26–28]. However, the Sivers function extracted from  $pp^\uparrow$  data with the twist-3 approach is shown to have a “sign mismatch” when compared to the Sivers function extracted from SIDIS data. The sign mismatch indicates a potential inconsistency in the current theoretical formalism [29] and needs to be further investigated. In order to understand the underlying mechanism producing TSSA it is crucial to study additional reaction channels [16,30].

In this Rapid Communication, we study TSSA from one of the experimentally least explored reactions, inclusive hadron production using a lepton beam on a transversely polarized nucleon ( $lN^\uparrow \rightarrow hX$ ) [16,31]. An early study of this process was done by Anselmino *et al.*, under the assumption that the underlying mechanism that generates TSSA is either the Collins or Sivers effects [31]. More recently, this study was re-evaluated using newly available SIDIS data on Sivers and Collins moments assuming that the TMD factorization is valid in  $lp^\uparrow \rightarrow \pi^\pm X$  processes at large  $p_T$  values. Due to the presence of only one hard scale in this process, estimation of the asymmetries is generally done at large  $p_T$  values (typically

\*kalyan@jlab.org

†Deceased.

$>1$  GeV/c). They predicted asymmetries between 5 and 10% for  $\sqrt{s} \simeq 4.9$  GeV,  $p_T = 1.5$  GeV/c, and  $x_F \leq 0.1$  with a contribution from the Sivvers mechanism to  $A_N$ , whereas the contribution from the Collins mechanism was negligible [16].

Nonzero SSAs were also estimated based on the twist-3 distribution and fragmentation functions in the framework of collinear factorization [30,32,33] and in the SIDIS process by integrating over the scattered electron's azimuthal angle [34]. These studies of TSSAs in the  $lp^\uparrow \rightarrow \pi^\pm X$  process are performed under the assumption of a SIDIS reaction, in which hard scattering occurs between a virtual photon and a quark. However, since the process is dominated by the cross section at  $Q^2$  near zero, it was also pointed out that the  $lp^\uparrow \rightarrow \pi^\pm X$  process will have significant contributions from soft processes, such as vector meson dominance, especially at lower  $p_T$  values [35]. Experimental data for TSSA in this process have recently been reported by the HERMES Collaboration using  $e^-/e^+$  beams on a transversely polarized hydrogen target [9].

We report the first measurement of target single-spin asymmetries ( $A_N$ ) in inclusive hadron ( $\pi^\pm$ ,  $K^\pm$ , and proton) production at fixed-target  $e + N$  center-of-mass energy  $\sqrt{s} = 3.45$  GeV, using an unpolarized electron beam and a transversely polarized  $^3\text{He}$  target as an effective polarized neutron target. The kinematical variables for this process are  $x_F = 2p^{c.m.}/\sqrt{s}$ , where  $p^{c.m.}$  is the momentum of the outgoing hadron along the polarized nucleon's momentum direction in the  $e + N$  center-of-mass frame, and  $p_T = \sqrt{p_x^2 + p_y^2}$ , the transverse momentum of the outgoing hadron. The kinematical configuration in the laboratory coordinate system is shown in Fig 1. The target spin “up”( $\uparrow$ ) was defined to be along the  $+\hat{y}$  direction, parallel to the vector  $\vec{l} \times \vec{P}_h$  ( $\phi_S = 90^\circ$ ), where  $\vec{l}$  and  $\vec{P}_h$  are the momentum vectors of the incoming beam and outgoing hadron, respectively.

The target SSA is defined as [16]

$$A_{UT}(x_F, p_T) = \frac{1}{P} \frac{d\sigma^\uparrow - d\sigma^\downarrow}{d\sigma^\uparrow + d\sigma^\downarrow} \sin\phi_S = A_N \sin\phi_S, \quad (1)$$

where  $d\sigma^{\uparrow(\downarrow)}$  is the differential cross section in the target “up”(“down”) state and  $P$  is the target polarization. The spin-dependent part of the cross section is proportional to the term  $\vec{S} \cdot (\vec{l} \times \vec{P}_h)$ , which gives rise to a  $\sin(\phi_S)$  modulation in the definition of the asymmetry. This term makes  $A_N$  parity

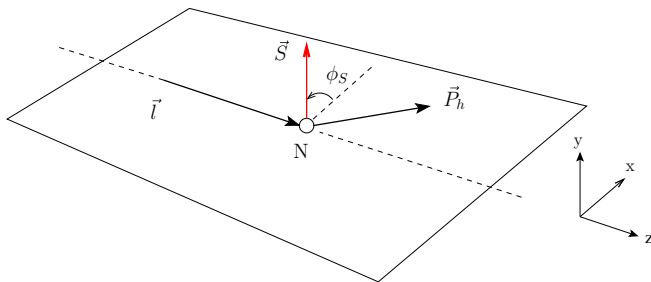


FIG. 1. (Color online) Kinematical configuration in the laboratory coordinate system for the  $lN^\uparrow \rightarrow hX$  process.  $\vec{P}_h$  represents the momentum direction of the produced hadron, and  $\vec{S}$  is the spin vector of the nucleon. The polarized nucleon's momentum is along the  $-z$  direction in the  $e + N$  center-of-mass frame.

conserving, but  $T$ -odd under “naïve” time reversal, in which the initial and final states do not interchange. Note that the sign of  $A_N$  in the laboratory coordinate system of this experiment [Eq. (1)] differs by a factor  $-1$  from the definition in the phenomenological study of this process in Ref. [16], where the authors used the center-of-mass coordinate system with the lepton moving in the  $-\hat{z}$  direction.

The data were collected using a singles trigger during the E06-010 experiment in Hall A at Jefferson Lab [36]. A beam energy of 5.9 GeV was provided by the CEBAF accelerator with an average current of  $12 \mu\text{A}$ . The produced hadrons were detected in a high-resolution spectrometer (HRS) [37] at a central angle of  $16^\circ$  on beam left side. Positively and negatively charged particles were detected separately by changing the magnet polarity of the HRS. The central momentum of the HRS was fixed at 2.35 GeV/c, with a momentum acceptance of  $\pm 4.5\%$  and solid angle of 6 msr. The average transverse momentum of the detected hadrons ( $\langle p_T \rangle$ ) was 0.64 GeV/c. We note that if the pions are produced through virtual or real-photon exchange ( $\gamma^* + N$  or  $\gamma + N$ ), the minimum photon energy is  $E_\gamma \geq 2.6$  GeV, corresponding to an invariant mass of  $W \geq 2.4$  GeV for the  $\gamma + N$  system, well above the region of nucleon resonances.

The data from the two helicity states from the polarized electron beam were summed over to achieve an unpolarized beam. The residual helicity-sorted beam-charge difference was less than 100 ppm in a typical run. The target spin direction was automatically reversed ( $\phi_S = \pm 90^\circ$ ) at a rate of once every 20 min, which allowed control of the combined systematic uncertainty due to luminosity fluctuations and time dependence to below 50 ppm in this experiment.

Polarized  $^3\text{He}$  targets have often been used as an effective polarized neutron targets, because in the ground state of the  $^3\text{He}$  nuclear wave function (dominated by the  $S$  state) the two proton spins are opposite to each other, and the nuclear spin is carried by the remaining neutron [38]. The polarized target used in this measurement was a 40-cm-long glass cell filled with  $\sim 8$  atm of  $^3\text{He}$  gas and a small amount ( $\sim 0.13$  atm) of  $\text{N}_2$  gas to reduce depolarizing effects [37]. The radiation lengths of the materials up to the center of the  $^3\text{He}$  target were Be window (0.072%),  $^4\text{He}$  gas (0.004%), glass window (0.142%), and  $^3\text{He}$  gas (0.046%). The target was polarized via hybrid spin-exchange optical pumping of a mixture of Rb-K [39]. The  $^3\text{He}$  polarization was measured every 20 min during the spin-reversal using nuclear magnetic resonance (NMR). The NMR signal was calibrated with electron paramagnetic resonance (EPR) measurements and a known NMR signal obtained from an identical water cell. The average in-beam polarization of the target was  $(55.4 \pm 2.8)\%$ .

The HRS detector package consisted of four separate detectors for particle identification: (i) a light-gas threshold Čerenkov for electron identification, (ii) a two-layer electromagnetic calorimeter for electron-hadron separation, (iii) a threshold aerogel Čerenkov detector for pion identification, and (iv) a ring imaging Čerenkov (RICH) detector for  $\pi^\pm$ ,  $K^\pm$ , and proton identification. The electron and positron background were suppressed with a rejection factor of  $10^4:1$ . After all the particle identification cuts the contamination due to leptons was negligible in the hadron sample. The pion

sample had a contamination of  $<1\%$  due to other hadrons. Kaons were identified using the RICH detector, in combination with a veto from the aerogel counter, to suppress the large pion background. To further improve the purity of the kaon sample, a  $\chi^2$  probability distribution was constructed based on the reconstructed Čerenkov ring angle and the expected Čerenkov angle in the RICH detector for a known particle momentum [40]. A cut on this distribution effectively suppresses the background events due to misidentified particles. The contamination of the kaon sample from other hadrons was estimated to be  $\sim 3\%$  (proton) and  $\sim 2\%$  ( $\pi^+$ ) for positive kaons, and  $\sim 2\%$  ( $\pi^-$ ) for negative kaons. Protons were identified using the same method that was used for charged kaons, producing a very clean sample with estimated background  $<1\%$ .

The raw  $^3\text{He}$  target single-spin asymmetry ( $A_N$ ) was obtained using the normalized yields in target spin up or down ( $\phi_S = \pm 90^\circ$ ) states, as shown in Eq. (1). The yield in each spin state is normalized with the accumulated beam charge and livetime of the data acquisition system in that state. The dilution of the measured  $^3\text{He}$  asymmetries due to the presence of a small amount of  $\text{N}_2$  gas in the target cell was corrected using the factor

$$f_{N_2} \equiv \frac{\rho_{N_2} \sigma_{N_2}}{\rho_{^3\text{He}} \sigma_{^3\text{He}} + \rho_{N_2} \sigma_{N_2}}, \quad (2)$$

where  $\rho$  is the density of the gas in the cell and  $\sigma$  is the unpolarized inclusive hadron cross section. The unpolarized  $\text{N}_2$  and  $^3\text{He}$  cross sections were obtained from the data taken during the experiment using reference cells filled with pure  $\text{N}_2$  and  $^3\text{He}$  gas. The  $f_{N_2}$  was extracted separately for all hadrons and was about  $\sim 10\%$  in each case.

The overall systematic uncertainty in this measurement was small due to frequent target spin flips. The false asymmetry due to luminosity fluctuations was less than  $0.04\%$  and was confirmed by measuring the target SSA in inclusive ( $e, e'$ ) DIS reaction for in-plane transverse target ( $\phi_S = 0^\circ, 180^\circ$ ). This configuration was achieved by rotating the target spin by  $90^\circ$  while keeping all other conditions the same. This type of asymmetry vanishes under parity conservation, assuming one-photon exchange. In addition, the inclusive pion asymmetry was measured to be zero with a precision of  $0.05\%$  in the same configuration ( $\phi_S = 0^\circ, 180^\circ$ ). This asymmetry is expected to vanish due to  $\sin(\phi_S)$  moment.

There were two additional sources of systematic uncertainty associated with the RICH detector for kaons and protons. The first one was from a cut on the number of hits in the RICH detector. The relative change in asymmetry under variation of the cut threshold was assigned as a systematic uncertainty. For  $K^\pm$  it was  $<14\%$  and for protons it was  $<3\%$ , relative to the statistical uncertainty. The second source was local fluctuations in the kaon and proton yields arising from detector inefficiencies in certain periods of the data collection. The systematic uncertainty was estimated using the change in the asymmetry obtained in the periods with and without these fluctuations and was estimated to be  $<2\%$ ,  $<6\%$ , and  $<1\%$ , relative to the statistical uncertainty, for  $K^+$ ,  $K^-$ , and protons, respectively. Systematic uncertainties due to the target density fluctuations, vertex cuts, data-acquisition (DAQ) livetime, and HRS single-track events were negligible.

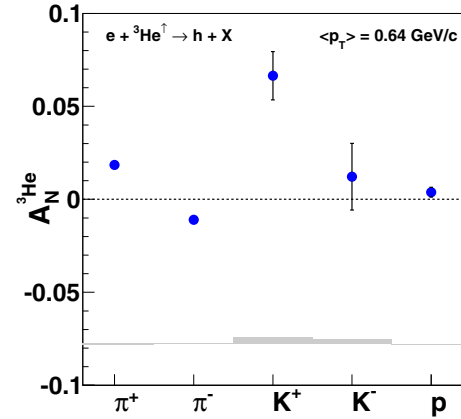


FIG. 2. (Color online) Inclusive SSA results on a  $^3\text{He}$  target for  $\pi^\pm$ ,  $K^\pm$ , and protons in the vertical target spin configuration ( $\phi_S = \pm 90^\circ$ ). The error bars on the points represent the statistical uncertainty. The gray band shows the magnitude of the overall systematic uncertainty for each hadron channel.

The final  $^3\text{He}$  asymmetry results are shown for different hadron species in Fig. 2. These results include a small correction due to particle contamination for each hadron species. In Fig. 2 the data were integrated in  $p_T$  and  $x_F$  (see Table I). The error bars represent the statistical uncertainty. The systematic uncertainties are shown as a solid band. The measured  $A_N$  for  $\pi^+$  ( $\sim 2\%$ ) and  $K^+$  ( $\sim 6\%$ ) are positive, and opposite in sign to that of  $\pi^-$  ( $\sim 1\%$ ). In addition, the magnitudes of these asymmetries follow  $|A^{\pi^-}| < |A^{\pi^+}| < |A^{K^+}|$ . The measured  $A_N$  for  $K^-$  and protons was found to be small and consistent with zero. We note that the majority of the detected protons originate through a knock-out reaction from the  $^3\text{He}$  nucleus, whereas mesons are produced either through fragmentation process or in a photoproduction reaction. The SSAs for charged pions as a function of  $p_T$  for a  $^3\text{He}$  target are shown in Fig. 3. The asymmetry grows as a function of  $p_T$  and plateaus around  $p_T \simeq 0.63 \text{ GeV}/c$ .

We extracted  $A_N$  on neutron from the measured  $^3\text{He}$  asymmetry using the effective polarization approach, previously used for both inclusive and semi-inclusive DIS processes [38,41]. Using this method,  $A_N$  for the neutron can be obtained

TABLE I. Central kinematics for three types of hadrons along with the  $A_N$  results for a  $^3\text{He}$  target. A negative  $x_F$  indicates that the produced hadron is moving backwards with respect to the nucleon momentum direction in the center-of-mass frame of the  $e + N$  system.

Hadron	$\langle x_F \rangle$	$\langle p_T \rangle$ (GeV/c)	$A_N^{^3\text{He}} \pm \text{Stat.} \pm \text{Sys.}$
$\pi^+$	-0.262	0.64	$0.0185 \pm 0.0007 \pm 0.0009$
$\pi^-$	-0.262	0.64	$-0.0109 \pm 0.0005 \pm 0.0005$
$K^+$	-0.215	0.64	$0.0665 \pm 0.0130 \pm 0.0038$
$K^-$	-0.215	0.64	$0.0122 \pm 0.0179 \pm 0.0027$
$p$	-0.087	0.64	$0.0038 \pm 0.0026 \pm 0.0002$

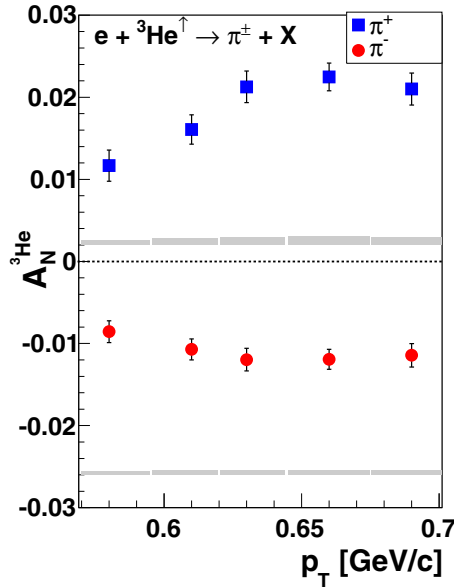


FIG. 3. (Color online)  $A_N$  results on a  ${}^3\text{He}$  target for the  $\pi^\pm$  channel as a function of  $p_T$ . The solid band on the bottom of each panel shows the magnitude of the systematic uncertainty for each momentum bin.

from  ${}^3\text{He}$  results using the relation

$$A_N^{3\text{He}} = P_n(1 - f_p)A_N^n + P_p f_p A_N^p, \quad (3)$$

where  $A_N^{3\text{He}}$  is the measured  ${}^3\text{He}$  asymmetry.  $P_n = 0.86^{+0.036}_{-0.02}$  and  $P_p = -0.028^{+0.009}_{-0.004}$  are the effective polarizations of the neutron and proton, respectively. Hence, the contribution of proton polarization ( $\simeq 2.8\%$ ) to  $A_N^{3\text{He}}$  is relatively small. The factor  $f_p = \frac{2\sigma_p}{\sigma_{3\text{He}}}$  in  ${}^3\text{He}$  was measured directly in this experiment using the yields obtained from unpolarized hydrogen and  ${}^3\text{He}$  targets. The average proton dilution  $(1 - f_p)$  for  $\pi^+$  was  $0.156 \pm 0.007$  and for  $\pi^-$  it was  $0.268 \pm 0.005$ . The SSA from a polarized proton target ( $A_N^p$ ) was assumed to be no more than  $\pm 5\%$  at  $p_T \simeq 0.64$  GeV/c, which is consistent with the HERMES data on  $A_N^p$  [9].

The final results for  $A_N^n$  for charged pions on an effective neutron target are shown in Fig. 4 and listed in Table II. The extracted  $A_N^n$  is below 20% for both  $\pi^+$  and  $\pi^-$ , with the asymmetry amplitude for  $\pi^+$  being larger than those for  $\pi^-$ . The  $A_N^n$  for both  $\pi^+$  and  $\pi^-$  increases up to  $p_T \simeq 0.63$  GeV/c, before it plateaus. Currently there are no theoretical estimates for  $A_N$  at  $\sqrt{s} = 3.45$  GeV and  $\langle p_T \rangle \sim 0.64$  GeV/c for a neutron

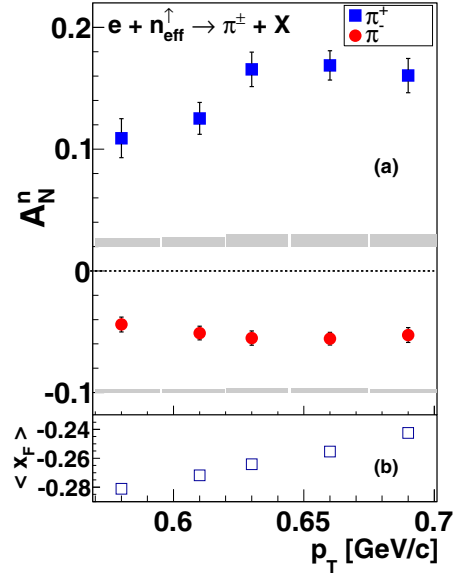


FIG. 4. (Color online) (a)  $A_N$  results on a neutron target extracted from the measured  ${}^3\text{He}$  asymmetries. The solid band on the bottom of each panel shows the magnitude of the systematic uncertainty for each momentum bin. The lower plot (b) is the  $x_F$  and  $p_T$  correlation in this measurement.

target. The existing predictions were done for a proton target at  $p_T = 1.5$  GeV/c and  $\sqrt{s} \simeq 4.9$  GeV [16]. However, the sign of  $A_N$  for  $\pi^\pm$  in our experiment is consistent with the existing predictions dominated by the Sivers effect, assuming  $p \leftrightarrow n$  and  $\pi^+ \leftrightarrow \pi^-$ .

We can compare the observed behavior of our data with existing TSSAs in both proton-proton ( $pp^\uparrow$ ) and lepton-nucleon ( $lN^\uparrow$ ) reaction channels. Our results show that in the center-of-mass frame of the polarized neutron-electron collision, viewed along the direction of the neutron's momentum,  $\pi^+$  favors the right side of the spin vector, whereas  $\pi^-$  favors the left side of the spin vector. Assuming isospin symmetry, this behavior is the same as that observed in  $pp^\uparrow \rightarrow hX$  for the E704 [2,3] and BRAHMS [4] experiments. In addition, this behavior is also the same as the Collins asymmetry for  $\pi^\pm$  and the Sivers asymmetry for  $\pi^+$  observed in SIDIS [6–8,12–14]. The  $A_N^n$  for  $\pi^+$  is about  $\sim 15\%$  at  $\langle p_T \rangle = 0.64$  GeV/c, which is larger than that for HERMES proton data for  $\pi^+$  ( $\sim 5\%$  at  $\langle p_T \rangle = 0.68$  GeV/c) [9]. Similarly, we observed large  $A_N^n$  for  $\pi^-$  ( $\sim 5\%$ ) compared to that for HERMES proton data ( $< 1\%$ ) [9]. Furthermore, we observed a large and positive amplitude

TABLE II. The extracted neutron  $A_N^n$  results for  $\pi^+$  and  $\pi^-$  along with their ratio  $R_{\pi^+/\pi^-}$  in five different  $\langle p_T \rangle$  bins.

$\langle p_T \rangle$ (GeV/c)	$A_N^n(\pi^+) \pm \text{Stat.} \pm \text{Sys.}$	$A_N^n(\pi^-) \pm \text{Stat.} \pm \text{Sys.}$	$R_{\pi^+/\pi^-}$
0.58	$0.109 \pm 0.016 \pm 0.007$	$-0.044 \pm 0.006 \pm 0.003$	$-2.5 \pm 0.5$
0.61	$0.125 \pm 0.013 \pm 0.008$	$-0.051 \pm 0.005 \pm 0.003$	$-2.5 \pm 0.4$
0.63	$0.166 \pm 0.014 \pm 0.010$	$-0.055 \pm 0.006 \pm 0.004$	$-3.0 \pm 0.5$
0.66	$0.169 \pm 0.012 \pm 0.010$	$-0.056 \pm 0.005 \pm 0.004$	$-3.0 \pm 0.4$
0.69	$0.160 \pm 0.014 \pm 0.010$	$-0.053 \pm 0.006 \pm 0.003$	$-3.0 \pm 0.5$

for the  $K^+$  asymmetry compared to  $K^-$  asymmetry on  $^3\text{He}$ , a similar feature observed in the  $lp^\uparrow \rightarrow hX$  reaction on proton target [9], and also the Sivers amplitude for kaons in the SIDIS reaction at HERMES [7].

In summary, we have reported the first measurement of SSAs in the inclusive hadron production reaction using unpolarized electrons on a transversely polarized  $^3\text{He}$  target at  $\langle p_T \rangle = 0.64$  GeV/c. Clear nonzero asymmetries were observed for charged pions and positive kaons, showing a feature of flavor dependence similar to that observed in the Sivers asymmetry in SIDIS, and in  $A_N$  in  $pp^\uparrow$  collisions. Currently there are no estimates or theoretical interpretations of these asymmetries at the relatively low  $p_T$  of 0.64 GeV/c used for this measurement. We hope that the results presented here will stimulate new theoretical and experimental efforts to pinpoint the exact origin of the

observed SSAs. Future experiments at Jefferson Lab [42,43], after the 12-GeV upgrade, will extend this measurement to higher values of  $p_T$  on both proton and  $^3\text{He}$  targets and will provide precision data for future theoretical studies. Moreover, if these nonzero asymmetries survive at high energy kinematics then they can be used as monitors of transverse target polarization in a fixed target experiment or local transverse polarization of the  $^3\text{He}$  beam at a future electron-ion collider.

We acknowledge the outstanding support of the JLab Hall A staff and the Accelerator Division in accomplishing this experiment. This work was supported in part by the U.S. National Science Foundation and Department of Energy (DOE) Contract No. DE-AC05-06OR23177, under which the Jefferson Science Associates operates the Thomas Jefferson National Accelerator Facility.

- 
- [1] V. Barone *et al.*, *Prog. Part. Nucl. Phys.* **65**, 267 (2010).  
 [2] D. Adams *et al.*, *Phys. Lett. B* **264**, 462 (1991).  
 [3] D. Adams *et al.*, *Phys. Lett. B* **261**, 201 (1991).  
 [4] I. Arsene *et al.*, *Phys. Rev. Lett.* **101**, 042001 (2008).  
 [5] B. I. Abelev *et al.*, *Phys. Rev. Lett.* **101**, 222001 (2008).  
 [6] A. Airapetian *et al.*, *Phys. Rev. Lett.* **94**, 012002 (2005).  
 [7] A. Airapetian *et al.*, *Phys. Rev. Lett.* **103**, 152002 (2009).  
 [8] A. Airapetian *et al.*, *Phys. Lett. B* **693**, 11 (2010).  
 [9] A. Airapetian *et al.*, *Phys. Lett. B* **728**, 183 (2014).  
 [10] M. G. Alekseev *et al.*, *Phys. Lett. B* **692**, 240 (2010).  
 [11] M. Alekseev *et al.*, *Phys. Lett. B* **673**, 127 (2009).  
 [12] C. Adolph *et al.*, *Phys. Lett. B* **717**, 376 (2012).  
 [13] C. Adolph *et al.*, *Phys. Lett. B* **717**, 383 (2012).  
 [14] X. Qian *et al.*, *Phys. Rev. Lett.* **107**, 072003 (2011).  
 [15] J. Huang *et al.*, *Phys. Rev. Lett.* **108**, 052001 (2012).  
 [16] M. Anselmino *et al.*, *Phys. Rev. D* **81**, 034007 (2010).  
 [17] J. Collins, *Nucl. Phys. B* **396**, 161 (1993).  
 [18] D. Sivers, *Phys. Rev. D* **41**, 83 (1990).  
 [19] S. J. Brodsky *et al.*, *Phys. Lett. B* **530**, 99 (2002).  
 [20] J. C. Collins, *Phys. Lett. B* **536**, 43 (2002).  
 [21] Z. Lu and I. Schmidt, *Phys. Rev. D* **75**, 073008 (2007).  
 [22] A. V. Efremov and O. Teryaev, *Sov. J. Nucl. Phys.* **36**, 140 (1982).  
 [23] A. Efremov and O. Teryaev, *Phys. Lett. B* **150**, 383 (1985).  
 [24] J. Qiu and G. Sterman, *Phys. Rev. Lett.* **67**, 2264 (1991).  
 [25] J. Qiu and G. Sterman, *Phys. Rev. D* **59**, 014004 (1998).  
 [26] X. Ji, J.-W. Qiu, W. Vogelsang, and F. Yuan, *Phys. Rev. Lett.* **97**, 082002 (2006).  
 [27] D. Boer *et al.*, *Nucl. Phys. B* **667**, 201 (2003).  
 [28] F. Yuan and J. Zhou, *Phys. Rev. Lett.* **103**, 052001 (2009).  
 [29] Z.-B. Kang, J.-W. Qiu, W. Vogelsang, and F. Yuan, *Phys. Rev. D* **83**, 094001 (2011).  
 [30] Z.-B. Kang, A. Metz, J.-W. Qiu, and J. Zhou, *Phys. Rev. D* **84**, 034046 (2011).  
 [31] M. Anselmino *et al.*, *Eur. Phys. J. C* **13**, 519 (2000).  
 [32] Y. Koike, *AIP Conf. Proc.* **675**, 449 (2003).  
 [33] Y. Koike, *Nucl. Phys. A* **721**, C364 (2003).  
 [34] B. Sun *et al.*, *Eur. Phys. J. C* **65**, 163 (2010).  
 [35] D. Sivers, *Phys. Rev. D* **43**, 261 (1991).  
 [36] K. Allada, Ph.D. thesis, University of Kentucky, 2010, [http://uknowledge.uky.edu/gradschool\\_diss/31/](http://uknowledge.uky.edu/gradschool_diss/31/)  
 [37] J. Alcorn *et al.*, *Nucl. Instrum. Meth. A* **522**, 294 (2004).  
 [38] F. Bissey, V. Guzey, M. Strikman, and A. Thomas, *Phys. Rev. C* **65**, 064317 (2002).  
 [39] E. Babcock, I. A. Nelson, S. Kadlecik, and T. G. Walker, *Phys. Rev. A* **71**, 013414 (2005).  
 [40] G. Urciuoli *et al.*, *Nucl. Instrum. Meth. A* **612**, 56 (2009).  
 [41] S. Scopetta, *Phys. Rev. D* **75**, 054005 (2007).  
 [42] K. Allada, *EPJ Web Conf.* **37**, 01028 (2012).  
 [43] "Jefferson laboratory experiments" [[http://wwwold.jlab.org/exp\\_prog/12GEV\\_EXP/](http://wwwold.jlab.org/exp_prog/12GEV_EXP/)], E12-09-018, E12-10-006, E12-11-108, E12-11-111.